



Optics Letters

Effect of p-doping on the intensity noise of epitaxial quantum dot lasers on silicon

JIANAN DUAN,^{1,*} YUEGUANG ZHOU,^{1,6} BOZHANG DONG,¹ HEMING HUANG,¹
JUSTIN C. NORMAN,^{2,3} DAEHWAN JUNG,^{3,5} ZEYU ZHANG,⁴ CHENG WANG,⁶
JOHN E. BOWERS,^{2,3,4} AND FRÉDÉRIC GRILLOT^{1,7}

¹LTCI, Télécom Paris, Institut Polytechnique de Paris, 19 place Marguerite Perey, 91120 Palaiseau, France

²Materials Department, University of California, Santa Barbara, California 93106, USA

³Institute for Energy Efficiency, University of California, Santa Barbara, California 93106, USA

⁴Department of Electrical and Computer Engineering, University of California Santa Barbara, Santa Barbara, California 93106, USA

⁵Center for Opto-electronic Materials and Devices, Korea Institute of Science and Technology, Seoul 02792, South Korea

⁶School of Information Science and Technology, Shanghai Tech University, Shanghai 201210, China

⁷Center for High Technology Materials, University of New Mexico, Albuquerque, New Mexico 87106, USA

*Corresponding author: jianan.duan@telecom-paristech.fr

Received 17 April 2020; revised 22 July 2020; accepted 3 August 2020; posted 4 August 2020 (Doc. ID 395499); published 31 August 2020

This work experimentally investigates the impact of p-doping on the relative intensity noise (RIN) properties and subsequently on the modulation properties of semiconductor quantum dot (QD) lasers epitaxially grown on silicon. Owing to the low threading dislocation density and the p-modulation doped GaAs barrier layer in the active region, the RIN level is found very stable with temperature with a minimum value of -150 dB/Hz. The dynamical features extracted from the RIN spectra show that p-doping between zero and 20 holes/dot strongly modifies the modulation properties and gain nonlinearities through increased internal losses in the active region and thereby hinders the maximum achievable bandwidth. Overall, this Letter is important for designing future high-speed and low-noise QD devices integrated in future photonic integrated circuits. © 2020 Optical Society of America

<https://doi.org/10.1364/OL.395499>

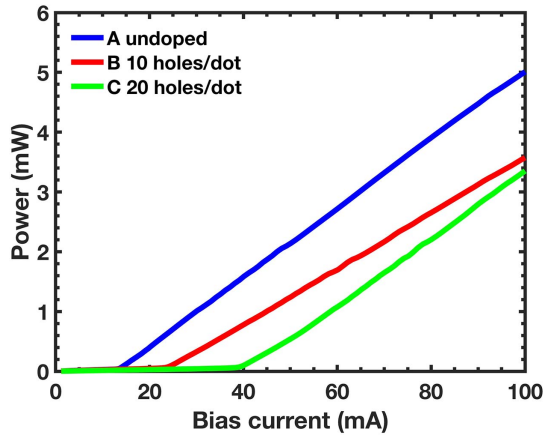
Due to their atom-like discrete energy levels, quantum dot (QD) lasers epitaxially grown on silicon are regarded as an excellent candidate to achieve energy and cost-efficient optical transceivers due to their outstanding properties such as high temperature stability, low threshold lasing operation, ultra-low frequency noise, high feedback tolerance, as well as low linewidth enhancement factor (α_H -factor) [1–4]. However, inhomogeneous broadening, enhanced nonlinear gain, as well as the population of carriers in the excited state are considered as the main limiting factors for the high-frequency response of QD lasers. To overcome these problems, p-type doping has been proposed to eliminate gain saturation and gain broadening due to hole thermalization [5,6]. In addition, the introduction of p-doping in the QD active region can further reduce the α_H -factor, which is beneficial for isolator-free integration [7]. Furthermore, optical transceivers with low relative intensity noise (RIN) are highly desired to carry broadband data with a

low bit error rate [8]. In the past few years, RIN values as low as -160 dB/Hz have been reported in both GaAs-based and InP-based QD lasers; however, the RIN values are found a bit higher between -120 dB/Hz and -150 dB/Hz in germanium and silicon substrate-based QD lasers [9–12]. Further improvement is envisioned by reducing the carrier noise originating from the ground and excited states or by increasing the energy interval between the quantum confined levels, which are even more suitable for low-intensity noise operation [13]. This Letter investigates the effect of p-doping on the RIN properties of QD lasers epitaxially grown on silicon. These experimental results show that the RIN level is very stable with temperature ranging from 15°C to 35°C for p-doped QD lasers. The minimal RIN values have been achieved between -140 dB/Hz and -150 dB/Hz for doping levels between zero and 20 holes/dot in the active region. In addition, dynamic properties are then extracted from the RIN spectra instead of using the laser's modulation response [8]. To this end, our results suggest an optimum doping level of 20 holes/dot for which the inverse of carrier lifetime, K -factor, and maximum modulation bandwidth are all improved, although at the price of a higher gain compression due to the increased internal losses.

The QD laser was grown on a GaP/Si template. The active region contains five periods of QD layers, each separated by a 37.5 nm GaAs spacer that includes 10 nm of p-type material. For p-modulation doped QD lasers, the 10 nm p-GaAs layer is doped with a target hole concentration of 0, $0.5 \times 10^{18} \text{ cm}^{-3}$, and $1 \times 10^{18} \text{ cm}^{-3}$. These doping concentrations correspond to zero, 10, and 20 extra holes per QD [14], labeled as devices A, B, and C, respectively, and listed in Table 1. Further details of the epitaxy growth are available elsewhere [15]. The Fabry–Perot (FP) cavities of the lasers are measured at similar lengths, 1.1 mm for the undoped devices and 1.35 mm for the p-doped devices, with 4 μm wide ridges deeply etched (through the active region), and two top contacts for electrical injection. The cavity facets are asymmetrically coated with power

Table 1. Static and Dynamic Characteristics of the Silicon-Based Undoped and p-Doped QD Lasers

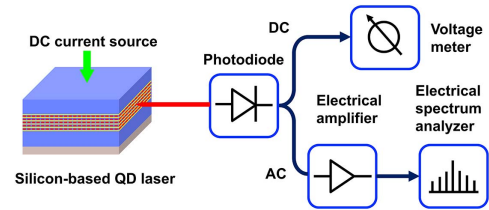
Device	A	B	C
Doping (cm ⁻³)	0	0.5 × 10 ¹⁸	1.0 × 10 ¹⁸
Holes per QD	0	10	20
I_{th} (mA)	13	23	39
J_{th} (A/cm ²)	296	426	722
K(ns)	4.7	1.7	1.5
γ_0 (GHz)	1.5	3.0	5.2
τ_c (ns)	0.7	0.3	0.2
$f_{3dB,max}$ (GHz)	1.9	5.2	5.9
ϵ_p (mW ⁻¹)	0.15	0.27	0.40
ϵ_s (cm ³)	5.7 × 10 ⁻¹⁶	1.0 × 10 ⁻¹⁵	1.5 × 10 ⁻¹⁵

**Fig. 1.** Light current characteristics of the QD lasers under study.

reflectivity of approximate 60% and 99% on the front and rear, respectively.

Figure 1 depicts the evolution of light current characteristics of the three QD lasers under study. At room temperature (20°C), the threshold current (I_{th}) for the undoped laser is 13 mA, while it increases from 23 mA (laser B) to 39 mA (laser C) with the increase in p-doping. The higher threshold of the p-doped lasers is due to the increased optical loss by high free carrier absorption that results from a large number of holes in the dots [16,17]. This high threshold current can be reduced by applying high-reflectivity coatings to both facets, which decreases the threshold gain requirements by a reduction in the mirror losses and hence promotes the low-threshold current [16]. On the other hand, it is known that the inclusion of p-type doping can mitigate the thermal spread of holes, leading to a rather temperature-insensitive threshold current [16,18,19]. All values of the I_{th} and the corresponding threshold current density J_{th} are summarized in Table 1.

Figure 2 shows the experimental setup for the measurement of the RIN. The silicon-based QD laser is pumped by a DC current source, while the device temperature is kept constant at 20°C using a thermo-electric cooler. The laser emission is coupled into a lensed fiber, and then the optical signal is converted into the electrical domain through a low-noise photodiode with a bandwidth of 10 GHz. The DC voltage is measured by a voltage meter through the DC monitor port of the photodiode, while the AC signal is amplified by a broadband amplifier with

**Fig. 2.** Experimental setup used for investigating the RIN of QD lasers.

a typical small-signal gain of 30 dB. In the end, the amplified noise spectrum is measured on an electrical spectrum analyzer (ESA). The intrinsic laser noise S_{Laser} can be expressed as

$$S_{Laser} = S_{Total} - S_{Thermal} - S_{Shot}, \quad (1)$$

where S_{Total} is the total noise measured by the ESA, $S_{Thermal}$ is the thermal noise independent of the optical power and determined when the laser is turned off, S_{Shot} is white noise determined by $S_{Shot} = 2qI_{DC}R_L$ with q the elementary charge, I_{DC} is the DC current, and R_L is the load resistance of the ESA. Overall, the RIN of the lasers can be recast as follows:

$$RIN = 10 \log_{10} \left[\frac{(S_{Total} - S_{Thermal}) / (RBW \times G) - S_{Shot}}{P_{DC}} \right], \quad (2)$$

with P_{DC} the electrical DC power, RBW the resolution bandwidth (200 kHz) of the ESA, and G the gain of the experimental setup including the amplifier, which is measured by the vector network analyzer (VNA). In order to ensure good accuracy, the RIN of a commercial quantum well (QW) is first measured, which is consistent with its RIN value of -138 dB/Hz at 10 GHz [20].

Figure 3 shows the measured RIN of the three tested QD lasers, which are extracted using Eq. (2). The RIN spectra are measured at various bias currents depending on their threshold currents. However, for better comparison, the three RIN spectra are measured for the same coupling power corresponding to the maximal limit of the photodiode (0.72 mW). The RIN at low frequencies is relatively high, resulting from the bias current noise, thermal noise, as well as mode partition [11], and it reduces with the increasing frequency and saturates at higher bias currents. The minimal RIN level is achieved between -140 dB/Hz and -150 dB/Hz in both undoped and p-doped lasers, which is also in agreement with results in Refs. [12,21]. The epitaxial defects in QD lasers accelerate the Shockley–Read–Hall (SRH) non-radiative recombination rate, which induces stronger photon variations and higher RIN compared with native QD lasers. Meanwhile, the fast non-radiative recombination shortens the total carrier lifetime and hence enhances the damping factor and decreases the relaxation oscillation frequency [22]. Figure 4 illustrates the averaged RIN values between 1 GHz and 4 GHz as a function of temperature ranging from 15°C to 35°C with a step of 5°C for undoped laser A and for p-doped laser B. For each temperature, the RIN values correspond to those taken at the same bias current, hence 90 mA for the undoped QD laser against 70 mA for the p-doped one. As shown in Fig. 4, the RIN values maintain the same level within the temperature range for the p-doped laser because the threshold current is rather constant with temperature. On the contrary, the RIN of the undoped laser increases

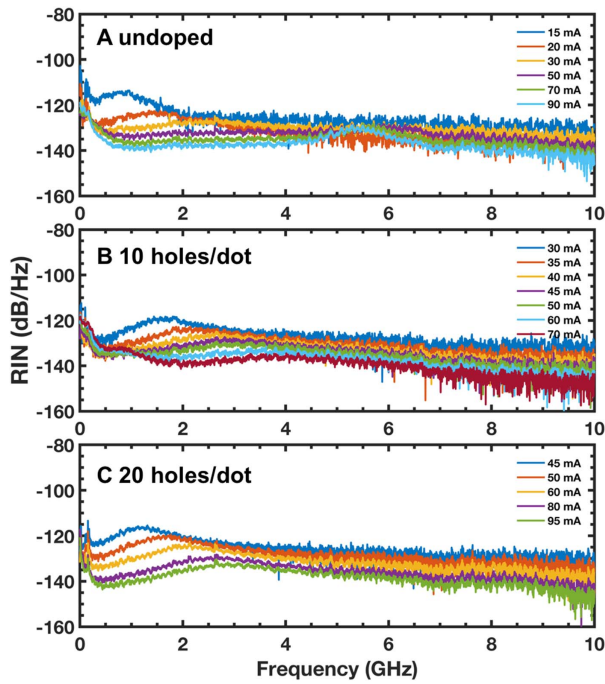


Fig. 3. RIN spectra up to 10 GHz for QD lasers A, B, and C, respectively.

from -140 dB/Hz at 15°C to -134 dB/Hz at 35°C . The p-doping can further improve the thermal performance with continuous-wave operation up to 105°C [23].

Moreover, Fig. 3 also shows that the RIN spectrum of undoped laser A exhibits a strong resonance peak at around 1 GHz, and it increases with the bias current as expected. At higher biases, the resonance peak vanishes at around 2 GHz, hence suggesting that the QD lasers are overdamped due to a large damping factor. On the other hand, p-doped lasers B and C exhibit a resonance frequency peak until higher biases, which results from an underdamping behavior due to a smaller damping factor.

In what follows, both the relaxation oscillation frequency (ROF) and damping factor are extracted from the curve-fitting of the RIN spectrum through the expression [8]

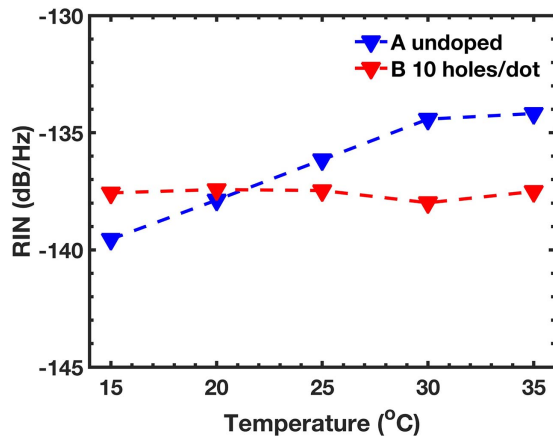


Fig. 4. Averaged RIN values between 1 GHz and 4 GHz as a function of temperature ranging from 15°C to 35°C with a step of 5°C for QD lasers A and B.

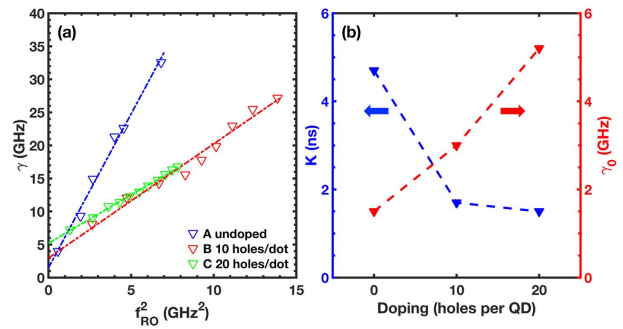


Fig. 5. (a) Measured damping factor (γ) as a function of the squared relaxation oscillation frequency (f_{RO}^2) for the QD lasers under study. (b) K -factor and inverse differential carrier lifetime (γ_0) versus the doping level.

$$\text{RIN}(\omega) = \frac{a + b\omega^2}{(\omega^2 - \omega_{\text{RO}}^2)^2 + \gamma^2\omega^2}, \quad (3)$$

with ω_{RO} the angular ROF, γ the damping factor, ω the angular frequency, and a and b coefficients used for the curve fitting. All dynamical parameters are summarized in Table 1. Figure 5(a) shows the damping factor as a function of the squared ROF for the three QD lasers, respectively. The evolution is linear following the relationship $\gamma = Kf_{\text{RO}}^2 + \gamma_0$ with K -factor, γ_0 is the damping factor offset associated with the inverse of the differential carrier lifetime (τ_c), and f_{RO} is the ROF. Figure 5(b) depicts the evolution of the K -factor and γ_0 extracted from the curve fitting as a function of the doping level. The K -factor decreases with the p-doping level from 4.7 ns (laser A) to 1.5 ns, the latter value corresponding to the optimum p-doping of 20 holes/dot (laser C), whereas γ_0 increases from 1.5 GHz to 5.2 GHz. The damping factor offset γ_0 is quite important at low powers where the ROF is small, while for larger resonance frequencies, the K -factor usually describes the damping of the response, which can be used to evaluate the maximum 3 dB bandwidth ($f_{3\text{dB,max}}$) from the following equation:

$$f_{3\text{dB,max}} = \frac{2\sqrt{2}\pi}{K}. \quad (4)$$

As expected, the calculated $f_{3\text{dB,max}}$ is 1.9 GHz for the undoped laser, which can be further increased to 5.9 GHz for the optimum p-doping level of 20 holes/dot. These results are consistent with previous works that showed that p-doping improves the maximum modulation bandwidth [18,24,25]. It is worthwhile to note that the obtained K -factors are similar to those calculated directly from the damping frequency $f_d \sim \epsilon_S S / 2\pi\tau_p = 2\pi/K$, with τ_p the photon lifetime, S the photon density, and ϵ_S the gain compression factor linked to the photon density [26,27]. Moreover, by varying the temperature, it is worth noting that the K -factor for undoped laser A is reduced from 4.7 ns at 20°C to 3.0 ns at 30°C . By comparison, the K -factor remains constant at both 20°C and 30°C for p-doped laser B, hence proving that the QD laser with p-doping is more stable over temperature [7].

The gain compression in QD lasers limits the modulation dynamics through adiabatic chirp effects, and it originates from gain nonlinearities caused by processes such as carrier heating and spatial and spectral hole burning [28]. In order to extract the gain compression factor, the evolution of the squared f_{RO} versus

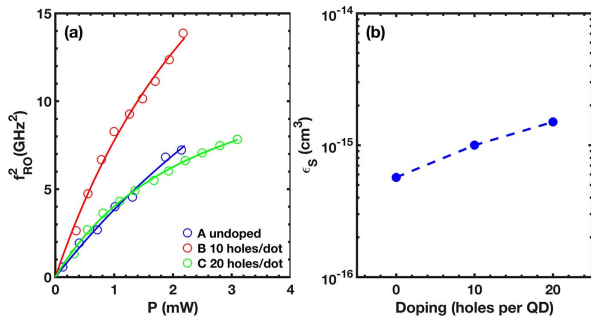


Fig. 6. (a) Squared relaxation oscillation frequency (f_{RO}^2) versus the output power (P) for the lasers under study. (b) Gain compression factor (ϵ_S) versus the doping level.

the output power (P) is plotted in Fig. 6(a) and curve-fitted using

$$f_{RO}^2 = \frac{AP}{1 + \epsilon_P P}, \quad (5)$$

with ϵ_P denoting the gain compression coefficient related to the output power P and A the modulation efficiency. By curve fitting the curves, ϵ_P is found to increase from 0.15 mW^{-1} for undoped laser A to 0.40 mW^{-1} for p-doped laser C. The gain compression factor linked to photon density (S) can then be expressed through the relationship $\epsilon_S = \epsilon_P P/S$, where $P = h\nu V v_g \alpha_m S$, V is the cavity volume, and $v_g \alpha_m$ is the energy loss through the mirrors. Taking into account the facet reflectivity and modal volume of the laser, Fig. 6(b) displays the calculated ϵ_S as a function of the doping level indicating values in the range from $5.7 \times 10^{-16} \text{ cm}^3$ to $1.5 \times 10^{-15} \text{ cm}^3$, which are in agreement with prior studies [28]. To conclude, the results show that the maximum modulation bandwidth and ROF can certainly be improved for doping levels between zero and 20 holes/dot beyond which no real improvements take place due to the joint effects of higher induced internal loss and gain nonlinearities [17,18,29].

To summarize, these experimental results show that the minimal RIN level below 10 GHz is achieved between -140 dB/Hz and -150 dB/Hz in both undoped and p-doped QD lasers and that p-doping increases the modulation bandwidth with doping levels between zero and 20 holes/dot. However, experiments also show that any further increase in p-doping enhances the gain compression effect due to increased internal losses, hence limiting the maximum achievable bandwidth in QD lasers. We believe that these novel insights are meaningful for designing future high-speed and low-noise QD devices to be integrated in future photonic integrated circuits (PICs). Last but not least, the high damping factor in QD lasers is also an important feature for isolator-free applications.

Funding. Advanced Research Projects Agency - Energy (DEAR0001039); Institut Mines-Telecom; National Natural Science Foundation of China (61804095).

Disclosures. The authors declare no conflicts of interest.

REFERENCES

- J. C. Norman, D. Jung, Z. Zhang, Y. Wan, S. Liu, C. Shang, R. W. Herrick, W. W. Chow, A. C. Gossard, and J. E. Bowers, *IEEE J. Quantum Electron.* **55**, 1 (2019).
- K. Nishi, K. Takemasa, M. Sugawara, and Y. Arakawa, *IEEE J. Sel. Top. Quantum Electron.* **23**, 1 (2017).
- W. W. Chow, Z. Zhang, J. C. Norman, S. Liu, and J. E. Bowers, *APL Photon.* **5**, 026101 (2020).
- J. Duan, H. Huang, B. Dong, D. Jung, J. C. Norman, J. E. Bowers, and F. Grillot, *IEEE Photon. Technol. Lett.* **31**, 345 (2019).
- D. G. Deppe, H. Huang, and O. B. Shchekin, *IEEE J. Quantum Electron.* **38**, 1587 (2002).
- O. Shchekin and D. Deppe, *Appl. Phys. Lett.* **80**, 2758 (2002).
- H. Huang, J. Duan, B. Dong, J. Norman, D. Jung, J. Bowers, and F. Grillot, *APL Photon.* **5**, 016103 (2020).
- L. A. Coldren, S. W. Corzine, and M. L. Mashanovitch, *Diode Lasers and Photonic Integrated Circuits* (Wiley, 2012), Vol. **218**.
- F. Lelarge, B. Dagens, J. Renaudier, R. Brenot, A. Accard, F. van Dijk, D. Make, O. Le Gouezigou, J.-G. Provost, F. Poingt, J. Landreau, O. Drisse, E. Derouin, B. Rousseau, F. Pommereau, and G.-H. Duan, *IEEE J. Sel. Top. Quantum Electron.* **13**, 111 (2007).
- A. Capua, L. Rozenfeld, V. Mikhelashvili, G. Eisenstein, M. Kuntz, M. Laemmlin, and D. Bimberg, *Opt. Express* **15**, 5388 (2007).
- Y.-G. Zhou, C. Zhou, C.-F. Cao, J.-B. Du, Q. Gong, and C. Wang, *Opt. Express* **25**, 28817 (2017).
- M. Liao, S. Chen, Z. Liu, Y. Wang, L. Ponnampalam, Z. Zhou, J. Wu, M. Tang, S. Shutts, Z. Liu, P. M. Smowton, S. Yu, A. Seeds, and H. Liu, *Photon. Res.* **6**, 1062 (2018).
- J. Duan, X.-G. Wang, Y.-G. Zhou, C. Wang, and F. Grillot, *IEEE J. Quantum Electron.* **54**, 1 (2018).
- Z. Zhang, D. Jung, J. Norman, W. W. Chow, and J. E. Bowers, *IEEE J. Sel. Top. Quantum Electron.* **25**, 1900509 (2019).
- D. Jung, J. Norman, M. J. Kennedy, C. Shang, B. Shin, Y. Wan, A. C. Gossard, and J. E. Bowers, *Appl. Phys. Lett.* **111**, 122107 (2017).
- M. T. Crowley, N. A. Naderi, H. Su, F. Grillot, and L. F. Lester, *Semiconductors and Semimetals* (Elsevier, 2012), Vol. **86**, pp. 371–417.
- J. C. Norman, Z. Zhang, D. Jung, C. Shang, M. Kennedy, M. Dumont, R. W. Herrick, A. C. Gossard, and J. E. Bowers, *IEEE J. Sel. Top. Quantum Electron.* **55**, 1 (2019).
- S. Hein, V. Von Hinten, S. Höfling, and A. Forchel, *Appl. Phys. Lett.* **92**, 011120 (2008).
- G. Ozgur, A. Demir, and D. G. Deppe, *IEEE J. Quantum Electron.* **45**, 1265 (2009).
- K. Petermann, *Laser Diode Modulation and Noise* (Springer, 2012), Vol. **3**.
- A. Y. Liu, T. Komljenovic, M. L. Davenport, A. C. Gossard, and J. E. Bowers, *Opt. Express* **25**, 9535 (2017).
- C. Wang and Y. Zhou, *J. Semicond.* **40**, 101306 (2019).
- D. Jung, J. Norman, Y. Wan, S. Liu, R. Herrick, J. Selvidge, K. Mukherjee, A. C. Gossard, and J. E. Bowers, *Phys. Status Solidi A* **216**, 1800602 (2019).
- R. R. Alexander, D. T. Childs, H. Agarwal, K. M. Groom, H.-Y. Liu, M. Hopkinson, R. A. Hogg, M. Ishida, T. Yamamoto, M. Sugawara, Y. Arakawa, T. J. Badcock, R. J. Royce, and D. J. Mowbray, *IEEE J. Quantum Electron.* **43**, 1129 (2007).
- K. Lüdge and E. Schöll, *Eur. Phys. J. D* **58**, 167 (2010).
- J. Helms and K. Petermann, *IEEE J. Quantum Electron.* **26**, 833 (1990).
- T. Ishikawa, R. Nagarajan, and J. Bowers, *Opt. Quantum Electron.* **26**, S805 (1994).
- F. Grillot, B. Dagens, J.-G. Provost, H. Su, and L. F. Lester, *IEEE J. Quantum Electron.* **44**, 946 (2008).
- A. Martinez, Y. Li, L. F. Lester, and A. L. Gray, *Appl. Phys. Lett.* **90**, 251101 (2007).